University of South Carolina
Scholar Commons

3-5-2007

Investigation of CdZnTe Crystal Defects Using Scanning Probe Microscopy

Goutam Koley
University of South Carolina - Columbia, koley@engr.sc.edu

J. Liu

K. C. Mandal
University of South Carolina - Columbia, mandalk@engr.sc.edu

Follow this and additional works at: https://scholarcommons.sc.edu/elct_facpub

Part of the [Electrical and Electronics Commons](#), and the [Engineering Physics Commons](#)

Investigation of CdZnTe crystal defects using scanning probe microscopy

G. Koley, J. Liu, and Krishna C. Mandal

Investigation of CdZnTe crystal defects using scanning probe microscopy

G. Koley[a)] and J. Liu
Department of Electrical Engineering, University of South Carolina, Columbia, South Carolina 29208

Krishna C. Mandal
EIC Laboratories, Inc., 111 Downey Street, Norwood, Massachusetts 02062

Surface electronic properties of $Cd_{0.9}Zn_{0.1}Te$ (CZT) crystals have been characterized using scanning spreading resistance microscopy (SSRM) and correlated with IR transmittance maps. SSRM performed on CZT samples showed excellent correlation with Te precipitates determined from infrared images. The average probe current was observed to be more than two orders of magnitude higher for the sample with higher Te precipitates. Stationary probe current-voltage relationship was found to be exponential and was modeled based on thermionic emission theory. Based on this model, the surface barriers of the CZT samples were found to be significantly different, which was confirmed independently from Kelvin probe measurements. © *2007 American Institute of Physics.*
[DOI: 10.1063/1.2712496]

$Cd_{0.9}Zn_{0.1}Te$ (CZT) materials have widespread applications in gamma-ray detectors, infrared focal plane arrays, environmental monitoring, high energy astrophysics, and medical imaging devices.[1–5] This is due to several interesting properties of these materials including large absorption coefficient, low bias voltage requirement, and room temperature operation. In spite of the excellent promise shown by these materials, the material quality has not been fully optimized. In particular, there are defects related to Te precipitates, which have been recently shown to significantly affect the device performance.[6] One of the major obstacles in the characterization of the Te precipitates is that they are often much smaller in size (less than 10 μm) compared to the probe beam diameters, which are usually on the order of 100 μm. Therefore, the correlation between the device performance and the Te precipitates is often not unequivocal. This has been clearly pointed out in a recent study by Carini *et al.*[7] Although a much better correlation was obtained in this study using improved probe beam diameter ($\sim$10 $\times$ 10 μm^2), it is still possible that Te precipitates with smaller dimensions (on the order of a few micrometers) may not be properly imaged. Therefore, for comprehensive evaluation and for mapping out the exact extent of the Te precipitates, a characterization technique with nanoscale resolution would be very attractive.

In this letter, we report the characterization results of scanning spreading resistance microscopy (SSRM) on CZT samples and the correlation between these images and infrared (IR) images of the samples as well as the electrical characteristics of the detector devices fabricated from them. Since it has been well established that the Te precipitates enhance the conductivity in the CZT samples, SSRM techniques would be quite appropriate to study high current regions in these samples, which may be correlated to Te precipitates. SSRM techniques with resolution of 10–20 nm are very well suited to extract the boundaries of these precipitates. One of the drawbacks of the SSRM characterization method is that it is only suitable for surface analysis. Nevertheless, important information can be obtained using this technique, since the Te precipitates are rather randomly distributed and many of them are expected to be exposed at the surface, especially after polishing and etching. Indeed, our results indicate that SSRM can be a very straightforward yet effective characterization tool for expedient determination of bulk CZT crystal quality.

In this study, measurements were performed on two CZT crystals with a large difference in Te precipitates (determined from the IR transmission maps). The crystals were grown by a specially modified vertical Bridgman technique, which has been reported elsewhere.[2] Simultaneous surface morphology and current images were obtained with *p*-type doped diamond probes using an Autoprobe M5 machine from Veeco. The probe current was measured using a current preamplifier (DL 1211) from DL Instruments. To establish Ohmic contacts, a Cr (20 nm)/Au (40 nm) metal stack was deposited on the back side of the samples.

The IR images (1×1 mm^2) of the two samples are shown in Fig. 1, where the black spots indicate the Te precipitates. Clearly the density of the Te precipitates is much lower in the first sample (to be called CZT1 from now on) than in the second sample (CZT2). Fabricated Frisch collar detectors showed higher dark leakage current (128 nA at −700 V bias) for the CZT2 sample compared to CZT1 (5.2 nA at −700 V bias). SSRM measurements were performed on both CZT1 and CZT2 samples to correlate the dark currents with the scanning probe currents. Simultaneously obtained surface morphology and probe current images on CZT1 are shown in Fig. 2. The morphology image shows a lot of scratch lines (depth ranging from a few na-
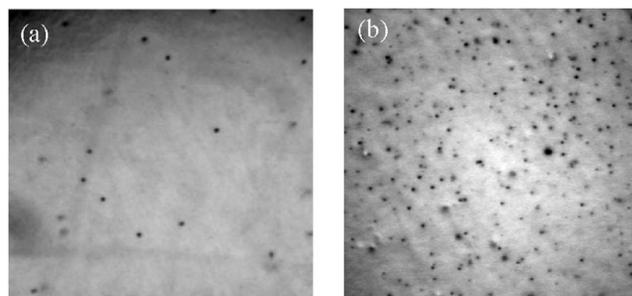

FIG. 1. IR transmission images (1×1 mm^2) of (a) CZT1 and (b) CZT2 crystals.
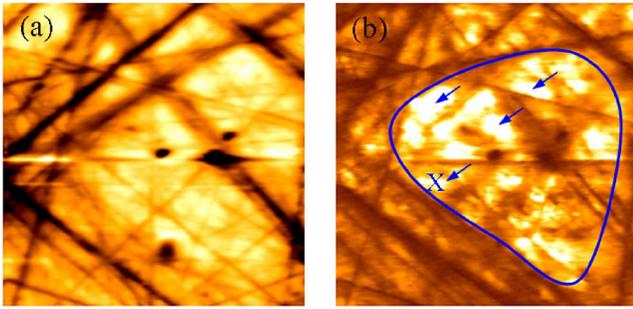
a)Electronic mail: koley@engr.sc.edu

FIG. 2. (Color online) (a) Surface morphology and (b) probe current images $(8 \times 8 \ \mu m^2)$ for the CZT1 crystal. The range of the scale bar for the current is 140 pA and that for the morphology is 60 nm. High current regions pointed with blue arrows are most likely regions of Te precipitate. The tip bias was maintained at −1.5 V for the current image. The "X" marked point is where stationary I-V measurements were performed.

FIG. 3. (Color online) (a) Topography and (b) probe current maps (8 $\times 8 \ \mu m^2$) for the CZT2 crystal. The range of the scale bar for the current is 2.5 nA and that for the morphology is 90 nm. High current regions are indicated by the blue arrows. The tip bias was maintained at −1.5 V for the current image. The "X" marked point is where stationary I-V measurements were performed.

nometers to tens of nanometers) arising from polishing of the crystal after growth. The current map has a lot of interesting features. We observe that there are certain areas [marked by blue arrows in Fig. 2(b)] where the current is much higher (reaches about 100 pA). Since the regions with Te precipitates are expected to have higher conductivity, these could be the areas where the Te precipitates are exposed at the surface due to polishing. The dimensions of the Te particles are somewhat difficult to estimate from the current maps. This is because the current decreases at the regions where there are scratches due to polishing, possibly due to surface and subsurface related damages. However, ignoring the scratch-related reduction in current, we can identify a roughly triangular area of high current (shown by the region bordered with blue line) with dimensions of 5−6 μm. These high current regions are quite isolated and sparse, supporting the low density of Te precipitates in this sample.

The surface morphology and the probe current maps for CZT2 are shown in Fig. 3. In comparison with CZT1, the current map of CZT2 [see Fig. 3(b)] shows a much higher (more than an order of magnitude) peak as well as an average current throughout the image. In addition, we do not see the well demarcated and isolated high current regions that were observed for CZT1 sample [Fig. 2(b)], rather a continuum of high current regions with some peaks is observed [marked by blue arrows in Fig. 3(b)]. Most likely this is due to the higher density of Te precipitates in this sample, leading to an averaging effect, since these precipitates were observed to influence the probe current even farther away from their physical location. This has also been observed for the probe current near the scratch marks, where the current is reduced even a few tenths of a micron away (from the scratch marks). Although at this point we are not sure of the exact reason behind these observations, it could be due to Debye length related carrier spreading.

For better comparison, stationary I-V measurements were performed on the high current regions of the two samples. For this measurement, the probe tip was positioned at the desired location (with zero scan size) and the current was measured while the voltage was swept from negative bias to positive bias (usually −1.7 to +1.7 V). The voltage sweep range was determined by the limit for instability and noise in the probe current. Single point I-V characteristics of the two samples [obtained at the "X" marked positions in Figs. 2(b) and 3(b)] are compared in Fig. 4. We notice that the I-V curves are very asymmetric, with negative probe bi-
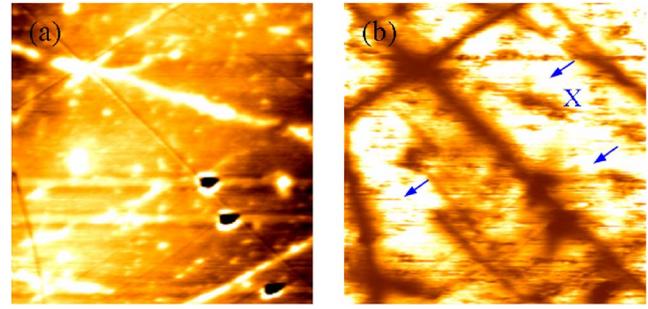
ases producing much higher current than positive biases. This behavior is consistent with the I-V characteristics on p-type doped samples.[8] Indeed Hall measurements performed on CZT2 indicate that the material is p type and the background majority carrier concentration of holes was measured to be $\sim 2 \times 10^{14} \ cm^{-3}$. The CZT1 sample was found to have a very high resistivity of $\sim 3 \times 10^{11} \ \Omega$ cm and the carrier type could not be determined from Hall measurements. Comparing Figs. 4(a) and 4(b), we also observed that the current for CZT2 at −1.5 V is more than two orders of magnitude higher than the current for CZT1 (12.5 nA and 56 pA, respectively). This is in agreement with our previous observation of a much higher probe current for CZT2 sample, as well as a much higher dark current in the Frisch collar detectors. From the logarithmic plots of the I-V curves, it can be seen that the I-V relationship is very nearly exponential for higher biases. However, the ideality factors for these curves were found to be extremely high ($\sim$18 for CZT1 and $\sim$16 for CZT2, calculated for the section of the I-V curve between V=1.2 and 1.5 V), which is nevertheless in agreement with previous observations of high nonideality factors in SSRM measurements on InP and GaAs samples[8] and can be expected for point contact systems.[9] The stationary probe current measured on CZT2 sample for a particular probe bias was found to be a few times higher than the scanning probe current for the same bias, most likely due to better contact formation.

The exponential behavior of the I-V characteristics can be explained by considering the thermionic emission mechanism for the current conduction, rather than simple resistive current flow, following the model proposed by Lu et al.[8] In their model, the probe current is limited by the interface potential barrier (giving rise to an exponential behavior), rather than the local doping level in the semiconductor (as in pure SSRM, where a linear I-V behavior is expected). The thermionic emission current in the forward bias (please note that for p-type doped sample, forward bias is established for negative tip voltage) is given as[8]

$$I_s = SA^{**}T^2 \exp\left(\frac{-q\phi_B}{k_BT}\right)\left\{\exp\left[\frac{q(V_a-\mathrm{IR}_s)}{nk_BT}\right]-1\right\}, \quad (1)$$

where A^{**} is the effective Richardson constant, S is the contact area, T is the temperature, ϕ_B is the surface barrier, and h, q, and k are Planck's constant, electronic charge, and Boltzmann's constant, respectively. In agreement with the earlier reports by Lu et al.,[8] the probe current magnitude in our
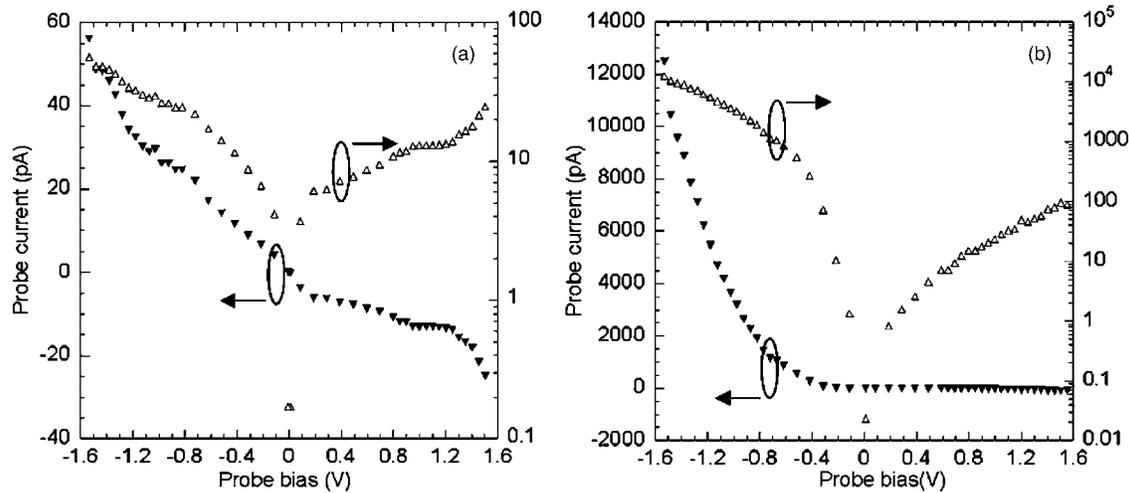
FIG. 4. (a) Stationary probe *I-V* measurements made on CZT1 at the point marked "X" in Fig. 2(b). (b) Stationary probe *I-V* measurements made on CZT2 at the point marked "X" in Fig. 3(b). Absolute values of the currents are displayed in logarithmic scale.

experiments is not very much dependent on the doping level, but is rather controlled by the surface barrier. Assuming that the series resistance R_s in Eq. (1) is negligible, at least for higher biases (a dominant series resistance leads to a linear *I-V* relationship, which is not observed), and other parameters remain the same, we can obtain the relationship between the currents, applied bias, and the surface barriers of the two samples as

$$\ln\left(\frac{I_{s,2}}{I_{s,1}}\right) = \frac{q}{k_B T}\left[(\phi_{B1} - \phi_{B2}) + \left(\frac{V_a}{n_2} - \frac{V_a}{n_1}\right)\right], \qquad (2)$$

where the subscripts 1 and 2 are used to denote quantities for CZT1 and CZT2 samples. For a tip bias of 1.5 V, the stationary probe current for CZT2 is approximately 220 times higher than that for CZT1 (12.5 nA compared to 56 pA). Neglecting the small difference in the ideality factors, the difference in surface barriers $(\phi_{B,1} - \phi_{B,2})$ calculated from Eq. (2) is ~0.14 eV. To independently verify this observation, Kelvin probe measurements were performed on the CZT1 and CZT2 samples using Au coated probes. Using Kelvin probe measurements, it is possible to measure the difference in surface work function (energy difference between the surface Fermi level and the vacuum level) of two samples $(V_{wf,1} - V_{wf,2})$, which is equal to the difference in the null (feedback) voltages $(V_{null,2} - V_{null,1})$ required to minimize electrostatic attractive force between the probe tip and the samples.[10,11] The null voltages for CZT1 and CZT2 samples (with the probe tip positioned sufficiently above the surface, following a measurement procedure described in detail in Ref. 12), were measured as ~750 and ~500 mV, respectively, indicating that the surface work function of CZT1 sample is lower than that of CZT2 by 0.25 eV. This also implies that the bare surface barrier height (BSBH), which for *p*-type materials is the energy difference between the Fermi level and valence band at the surface, for CZT1 is higher than that for CZT2 by 0.25 eV. The difference in BSBH for the two samples is higher than the barrier height difference estimated from Eq. (2), based on measurements performed with the probe in contact with the sample surface. However, this is not totally unexpected since the BSBH values are usually larger than the surface barrier measured at a contact due to the effects of the surface states (Sze-Cowley model).[12]

In conclusion, we have used the SSRM technique to characterize the surface electronic properties of CZT semiconductor materials. We have demonstrated the usefulness of this technique for the characterization of CZT samples, especially the extent of Te precipitate, which determines the average background carrier concentration in these samples. The characterization results obtained by the SSRM technique were found to be in complete agreement with the results of IR transmittance images and dark currents measured in Frisch collar detectors fabricated from these samples. The sample with higher density of Te precipitate was found to have its surface barrier lowered significantly, which was confirmed independently by Kelvin probe measurements.

[1]R. B. James, T. E. Schlesinger, J. C. Lund, and M. Schieber, *Semiconductors for Room Temperature Nuclear Detector Applications* (Academic, New York, 1995), Vol. 43, p. 334..

[2]K. C. Mandal, S. H. Kang, M. Choi, J. Bello, L. Zheng, H. Zhang, M. Groza, U. N. Roy, A. Burger, G. E. Jellison, D. E. Holcomb, G. W. Wright, and J. A. Williams, J. Electron. Mater. **35**, 1251 (2006).

[3]S. Sen, H. L. Hettich, D. R. Rhiger, S. L. Price, M. C. Currie, R. P. Ginn, and E. O. McLean, J. Electron. Mater. **28**, 718 (1999).

[4]G. A. Carini, A. E. Bolotnikov, G. S. Camarda, G. W. Wright, G. De Geronimo, D. P. Siddons, and R. B. James, IEEE Trans. Nucl. Sci. **52**, 1941 (2005).

[5]A. Burger, M. Groza, Y. Cui, U. N. Roy, D. Hillman, M. Guo, L. Li, G. W. Wright, and R. B. James, Phys. Status Solidi C **2**, 1586 (2005).

[6]A. E. Bolotnikov, G. S. Camarda, G. A. Carini, M. Fiederle, L. Li, D. S. McGregor, W. McNeil, G. W. Wright, and R. B. James, IEEE Trans. Nucl. Sci. **53**, 607 (2006).

[7]G. A. Carini, A. E. Bolotnikov, G. S. Camarda, G. W. Wright, R. B. James, and L. Li, Appl. Phys. Lett. **88**, 143515 (2006).

[8]R. P. Lu, K. L. Kavanagh, St. J. Dixon-Warren, A. J. SpringThorpe, R. Streater, and I. Calder, J. Vac. Sci. Technol. B **20**, 1682 (2002).

[9]R. J. Hillard, R. G. Mazur, H. L. Berkowitz, and P. Rai Choudhury, Solid State Technol. **32**, 119 (1989).

[10]G. Koley and M. G. Spencer, J. Appl. Phys. **90**, 337 (2001).

[11]G. Koley and M. G. Spencer, *Encyclopedia of Nanoscience and Nanotechnology* (American Scientific, Stevenson Ranch, 2003), Vol. 4, p. 327.

[12]S. M. Sze, *Physics of Semiconductor Devices*, 2nd ed. (Wiley, New York, 1981), p. 273.